Journal of Bioscience and Bioengineering
VOL. 125 No. 4, 479–489, 2018

ELSEVIER

www.elsevier.com/locate/jbiosc

Deciphering defective amelogenesis using *in vitro* culture systems

Dian Yosi Arinawati,[1] Keiko Miyoshi,[2] Ayako Tanimura,[2] Taigo Horiguchi,[2] Hiroko Hagita,[2] and Takafumi Noma[2,*]

Graduate School of Oral Sciences, Tokushima University, 3-18-15 Kuramoto, Tokushima 770-8504, Japan[1] and Department of Molecular Biology, Institute of Biomedical Sciences, Tokushima University Graduate School, 3-18-15 Kuramoto, Tokushima 770-8504, Japan[2]

Received 22 September 2017; accepted 16 November 2017
Available online 1 February 2018

The conventional two-dimensional (2D) *in vitro* culture system is frequently used to analyze the gene expression with or without extracellular signals. However, the cells derived from primary culture and cell lines frequently deviate the gene expression profile compared to the corresponding *in vivo* samples, which sometimes misleads the actual gene regulation *in vivo*. To overcome this gap, we developed the comparative 2D and 3D *in vitro* culture systems and applied them to the genetic study of amelogenesis imperfecta (AI) as a model. Recently, we found specificity protein 6 (*Sp6*) mutation in an autosomal-recessive AI rat that was previously named AMI. We constructed 3D structure of ARE-B30 cells (AMI-derived rat dental epithelial cells) or G5 (control wild type cells) combined with RPC-C2A cells (rat pulp cell line) separated by the collagen membrane, while in 2D structure, ARE-B30 or G5 was cultured with or without the collagen membrane. Comparative analysis of amelogenesis-related gene expression in ARE-B30 and G5 using our 2D and 3D *in vitro* systems revealed distinct expression profiles, showing the causative outcomes. Bone morphogenetic protein 2 and follistatin were reciprocally expressed in G5, but not in ARE-B30 cells. All-or-none expression of amelotin, kallikrein-related peptidase 4, and nerve growth factor receptor was observed in both cell types. In conclusion, our *in vitro* culture systems detected the phenotypical differences in the expression of the stage-specific amelogenesis-related genes. Parallel analysis with 2D and 3D culture systems may provide a platform to understand the molecular basis for defective amelogenesis caused by *Sp6* mutation.

[**Key words:** Amelogenesis imperfecta; Cell–cell interaction; Cell–matrix interaction; Dental epithelial cell; Genetic disease; *In vitro* amelogenesis imperfecta model; Phenotypic screening; *Sp6*]

An *in vitro* cell culture system is frequently utilized to understand the molecular mechanism of the biological events *in vivo* such as cell growth, differentiation, or cell death (1). The advantage of conventional 2D culture is simple and easy to manipulate cultural conditions by controlling supplements or treatments. However, the disadvantage is unable to phenocopy morphological and physiological status including gene expression *in vivo* (2,3). On the other hand, several 3D culture systems have been reported using combination of cellular distribution, extracellular contacts, specific nutrient and growth factor additions by mimicking physiological situation *in vivo* although their standardization remains to be established (2,4). Based on these considerations, we developed the comparative 2D and 3D *in vitro* culture systems and applied them to the genetic study of amelogenesis imperfecta (AI) associated with specificity protein 6 (*Sp6* also known as epiprofin) mutation.

AI is a hereditary complex disorder, which exhibits defects in enamel formation (5). Based on its structure and clinical appearance AI is originally classified into the following five phenotypes: hypoplastic, hypocalcification, hypomaturation, pigmented hypomaturation, and local hypoplasia (5,6). Recent genetic studies on AI-causative genes have revealed genotype–phenotype correlations, and partly clarified the mechanisms involved in amelogenesis (7). However, a comprehensive understanding about the entire process of amelogenesis and the regulatory factors involved remains to be achieved.

Amelogenesis is the process of enamel formation and mineralization, and comprises the secretory, transition, maturation, and post-maturation stages, concomitant with ameloblast differentiation (7). At the initiation stage, dental epithelium (inner enamel epithelium, IEE) and mesenchyme are separated by the basement membrane. However, during the pre-secretory stage, odontoblasts secrete a matrix composed mainly of type I collagen (pre-dentin), which is followed by the degradation of the basement membrane by matrix metallopeptidases (MMPs) (8,9). Consequently, the pre-ameloblasts come in direct contact with the pre-dentin and the odontoblasts, and differentiate into ameloblasts. The ameloblasts deposit enamel matrix proteins including ameloblastin (Ambn), enamelin (Enam), and amelogenin (Amel) during the secretory stage. Mmp20, one of the enamel proteinases, is also secreted at this stage (10). After passing through the transition stage, characterized by reduced protein secretion and ameloblast remodeling, the maturation stage (final stage) is reached, wherein the enamel matrix is replaced with mature enamel by matrix protein degradation, ion transport, and complete crystallization of the enamel (7,10,11). Kallikrein-related peptidase 4 (Klk4) and amelotin (Amtn) are secreted during the transition and maturation stages (12,13). Klk4, instead of Mmp20, further degrades the enamel matrix

* Corresponding author. Tel./fax: +81 88 633 7326.
E-mail address: ntaka@tokushima-u.ac.jp (T. Noma).

1389-1723/$ – see front matter
https://doi.org/10.1016/j.jbiosc.2017.11.009

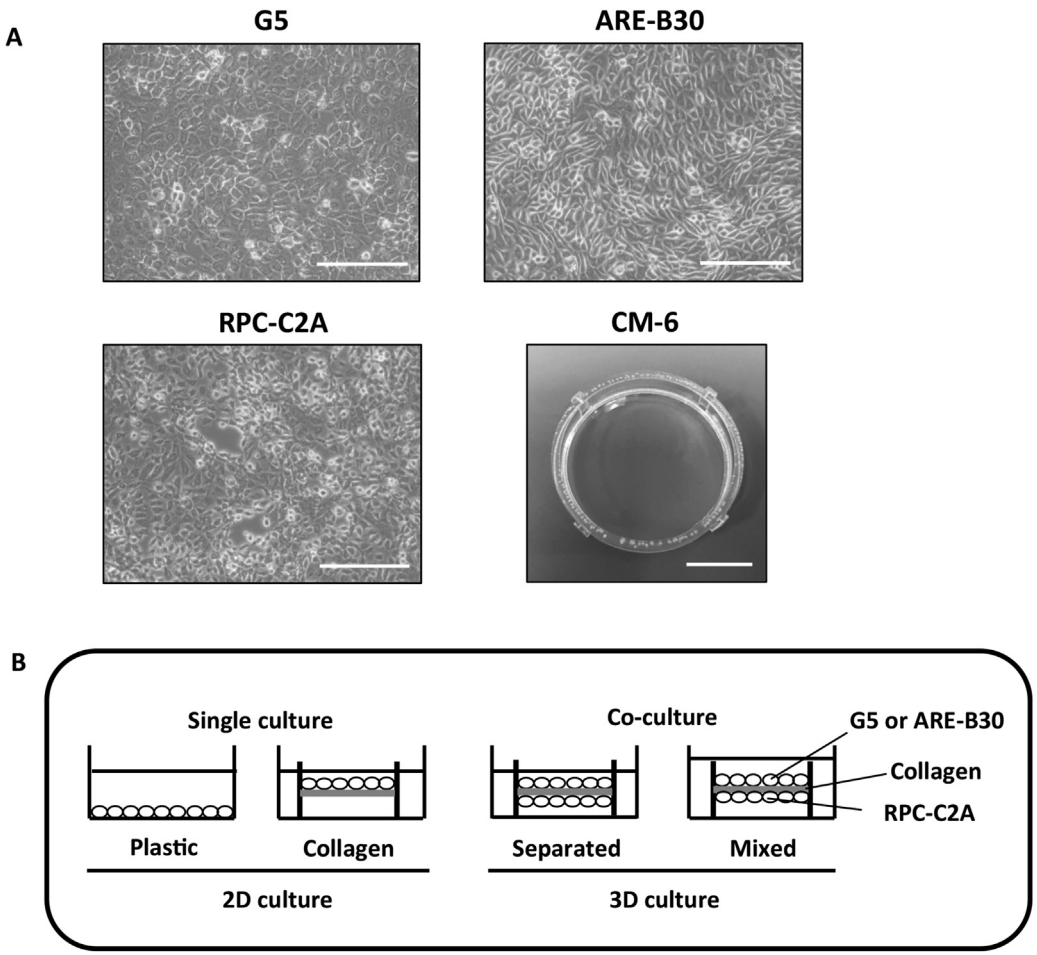

FIG. 1. Cell morphology and design of the cell culture system. (A) Appearance of cells and the collagen membrane device. Bars indicate 0.25 mm for G5, ARE-B30, and RPC-C2A, and 1 cm for CM-6, respectively. (B) Design of the culture systems. The details are described in text.

proteins and controls cellular signaling (14), whereas Amtn is suggested to play a role in cell–matrix attachment and mineral nucleation in order to promote mineralization (7,15). Hence, a simplified *in vitro* model system of amelogenesis is required to analyze and understand the complex processes involved in AI.

AMI has been reported as a spontaneous AI rat model with autosomal-recessive inheritance (16). Recently, we found AMI has a 2-base-insertional mutation in *Sp6*, resulting a truncation in the 3rd zinc-finger domain of Sp6, which was genetically linked to AI phenotype (17). According to the tissue distribution of *Sp6* mRNA in teeth, hair follicles, embryonic limb buds, and adult lung (18,19), *Sp6*-deficient mice showed defective tooth morphogenesis and development together with other systemic phenotypes (19,20). In contrast, the *Sp6*-mutated AMI rat presented with enamel defects only (17), making it a simplified model to study Sp6 function in amelogenesis. To restore the AMI phenotype, we developed the *Sp6* transgenic rat and mated it with an AMI rat. However, although complete rescue of the AMI phenotype was not obtained, partial morphological restoration in dental epithelial cells during tooth development was effected (21). Hence, to understand the mechanistic correlation between *Sp6* mutation and AI, we established a dental epithelial cell clone derived from AMI (ARE-B30), which was used as an *in vitro* AI model (22).

Until now, we have reported several characteristics of the Sp6 gene and protein using the wild-type rat-derived control clone, G5 (23–25). *Sp6* is composed of three exons, and is transcribed by two promoters along with a potential third promoter in a cell type-specific manner (24). The second *Sp6* promoter is negatively regulated by chicken ovalbumin upstream promoter transcription factor-interacting protein 2 (Ctip2, also known as Bcl11b), a known upstream regulator for *Sp6* (26). Sp6 protein expression was detected in the pre-ameloblast to maturation stages during amelogenesis by immunohistochemical analysis (27). Thereby, we have proposed that Sp6 may play a dual role in ameloblast differentiation. It negatively regulates follistatin (*Fst*) gene expression, which inhibits the bone morphogenetic protein (BMP)-axis during ameloblast differentiation (27), and positively regulates the expression of Rho-associated coiled-coil containing protein kinase 1 (*Rock1*) gene (28), which is an important regulator of cell polarity in amelogenesis (29). Sp6 is a short-lived protein regulated by a proteasomal system in dental epithelial cells; hence, stabilization of Sp6 is required for the normal functioning of these cells (25). Collectively, our findings indicated that Sp6 function is tightly regulated in a spatio-temporal manner.

In the present study, we aimed to analyze the molecular basis for the genotype and phenotype correlation in an *in vitro* AI model with *Sp6* mutation. Two-D and 3D culture systems were established *in vitro* to mimic the stages of amelogenesis that occur *in vivo*, and the comparative phenotypic screening clearly revealed distinct defective amelogenesis.

MATERIALS AND METHODS

Cell culture Rat dental epithelia-derived cells, G5 (23), and AI rat-derived dental epithelial cells, ARE-B30 (22), were cultured in Dulbecco's modified Eagle's

TABLE 1. Sequences of primer sets for RT-PCR.

Gene	Primer sequence (5′ → 3′)	Product size (bp)
Sp6-WT	CGGTCTGCAGCCGTGTC	195
	ACATCCATGGGGCTCAGTTG	
Sp6-AMI	GGTCTGCAGCCGTGTGTC	196
	ACATCCATGGGGCTCAGTTG	
Cdh1	CGTGATGAAGGTCTCAGCC	615
	ATGGGGGCTTCATTCACGTC	
Bmp2	TGAACACAGCTGGTCTCAGG	343
	GCTAAGCTCAGTGGGGACAC	
Fst	TTTTCTGTCCACCGGCAGCTCCAC	437
	GCAAGATCCGGAGTGCTTCACT	
Ngfr	TGTGTGAAGAGTGCCCAGAG	496
	TCCACAGAGATGCCACTGTC	
Mmp20	TGTGGAGTTCCTGATGTGGC	426
	TGATGGGTCTGTGGAATGGC	
Klk4	CTTCTTTTGCCAACGACCTC	429
	TTGTCTGAATGGTGGTCCAG	
Amtn	CCTCCTTATCCACCCCTTG	296
	CCAACTGTGATGTGGTTTGC	
18s rRNA	TACCTGGTTGATCCTGCCAGTAGGAT	185
	CCCGTCGGCATGTATTAGCTCTAGAA	

medium/Hams'F12 medium (D/F12; Nissui, Tokyo, Japan) supplemented with 10% fetal bovine serum (FBS; JRH Biosciences, Lanexa, KS, USA). Rat dental pulp cells, RPC-C2A (30), were cultured in Eagle's minimum essential medium (Nissui) supplemented with 10% FBS. All cells were incubated at 37 °C in 5% CO_2 atmosphere, and passaged every three days. Cellular morphologies are shown in Fig. 1A.

Two-D culture systems Two types of 2D culture systems were prepared. G5 or ARE-B30 was seeded on a 35 mm plastic culture dish (Corning Life Sciences, Durham, NC, USA), or a collagen membrane (CM-6; Koken, Tokyo, Japan) (Fig. 1A). CM-6 was used for the extracellular matrix (ECM). The small molecules less than 20 kDa can be passed through this membrane according to the product information.

Three-D culture systems using collagen type I membrane To establish an *in vitro* 3D culture system, we modified the previously reported system (31) using dental epithelial and dental pulp cell-lines derived from the same species (rat). RPC-C2A cells, which endogenously express *Bmp2* and *Bmp4* mRNA and exhibit mineralizing activity (32), were seeded onto one side of the CM-6 placed in a well in a 6-well cell culture plate (Corning Life Sciences). After 12 h, the cells were washed in PBS (−) to remove the non-attached cells. The CM-6 was reversed and placed into another well of a 6-well plate; G5 or ARE-B30 cells was then seeded onto this side of the CM-6 and cultured for 5 h. The membrane was washed in PBS (−) to remove the non-attached cells. Finally, the CM-6 was transferred to a new plate, fresh medium was added, and the culturing process was started (time 0).

The 3D culture system was maintained with two different volumes of culture medium. First, the culture medium for the RPC-C2A cells was added into each well of the culture plate, while the media for the G5 or ARE-B30 cells were added separately into the CM-6 device (separated medium). Second, the culture medium was added into the well of the culture plate until it came in contact with the culture medium inside the CM-6 device (mixed medium). The number of cells seeded was 6.0×10^5 cells/well, which reached 100% confluency by day 1. The cells were cultured in D/F12 medium with 10% FBS for 1–14 days. The culture medium was changed every 2 days.

Effects of cell density G5 cells were seeded onto a 35 mm plastic dish at 3×10^4; 1×10^5; 3×10^5; 1×10^6 cells per dish corresponding to the confluency of the cells at 3%, 10%, 30% and 100%, respectively, at day 1. The cells were harvested for RNA isolation at day 1, day 3, and day 5 after seeding. Culture media were changed every 2 days.

Reverse transcription-polymerase chain reaction Total RNA was isolated from each sample at the indicated time points using the TRI reagent (Molecular Research Center, Cincinnati, OH, USA) and treated with DNase I (Invitrogen, Life Technologies, Carlsbad, CA, USA) according to manufacturer's protocols. Complementary DNA was obtained by reverse transcription using random primers and the RNA PCR kit AMV (version 3.0; Takara Bio Inc., Otsu, Japan), according to the manufacturer's protocol. The mRNA levels of ameloblast differentiation marker genes were analyzed by reverse transcription-polymerase chain reaction (RT-PCR) using GoTaq DNA polymerase (Promega, Madison, WI, USA). PCR products were detected by agarose gel electrophoresis. The gene-specific primer sets used in this study are listed in Table 1. The expression level of each mRNA was normalized to that of *18S rRNA*.

Densitometric analysis Signals from the RT-PCR products were captured by ChemiDoc XRS (Bio-Rad Laboratories, Segrate, Milan, Italy), and their intensities were analyzed using a software application Quantity One (Bio-Rad). The relative expression level of each gene was calculated against the positive control (denoted as 1).

Statistical analysis Student's *t*-test was performed using the excel software (Microsoft Excel 2010, Microsoft).

RESULTS

Establishment of an *in vitro* culture system that mimics amelogenesis *in vivo* Four different culture systems were prepared (two for the 2D and two for the 3D systems) as shown in Fig. 1B. In this study, we defined 2D refers to the two components; epithelial cells and matrix. Similarly, 3D refers to the three components; epithelial cells, matrix, and mesenchymal cells, which mimics the *in vivo* structure. The 2D culture systems comprised two types of culture conditions; the first system involved the culture of either G5 or ARE-B30 on the conventional plastic dish (hereafter, plastic culture), whereas in the second system, G5 or ARE-B30 were cultured on the collagen membrane (hereafter, collagen culture). For 3D culture systems, two different conditions were set up. To examine the paracrine effects of mesenchymal cells through the collagen membrane (less than 20 kDa molecules can be passed), the third system involved the co-culture of either G5 or ARE-B30 with RPC-C2A on the collagen membrane in a separated medium (hereafter, separated culture). The culture conditions in the fourth system were similar to that of the third system, except for the connection of the culture media between the epithelial side and the mesenchymal side (hereafter, mixed culture). In the fourth culture system, the soluble factor(s) derived from the mesenchymal cells can be provided to the epithelial cells through the culture medium, and the autocrine and paracrine effects of soluble factor(s) from epithelial cells can be diluted (Fig. 1B).

Expression of regulatory molecules in epithelial cells during amelogenesis Stage-specific biomarkers of ameloblasts *in vivo* were used to recognize the progress in cellular differentiation corresponding to amelogenesis (Fig. 2A). The mRNA expression levels of several ameloblast differentiation marker genes were analyzed by semi-quantitative RT-PCR (Fig. 2B–D). The expression levels of *Sp6* and cadherin 1 (*Cdh1*, also known as *E-cad*), representing the general markers of dental epithelial cells, were examined to confirm the basic characteristics of G5 and ARE-B30. As illustrated in Fig. 2A, *Sp6* mRNA expression has been detected predominantly in the mouse dental epithelium during all stages of ameloblast differentiation (18). We designed two specific primer sets, namely *Sp6WT* and *Sp6AMI*, to evaluate the expression of wild- or mutant-type *Sp6*. Similar levels of *Sp6* mRNA expression were observed in both G5 and ARE-B30 cells from day 1 to day 14 among all the culture systems (Fig. 2B, a and b). In addition, *Cdh1* expression was examined during culture because previous studies have reported the expression of this gene during all stages of ameloblast differentiation (33). Both G5 and ARE-B30 expressed *Cdh1* with no gross changes among the culture systems and the various time courses, confirming that both cells had maintained their epithelial identities (Fig. 2B).

Next, we analyzed the regulatory molecules of amelogenesis. As seen in Fig. 2A, previous studies have demonstrated the reciprocal expression patterns of *Bmps* and *Fst* during the initiation, secretory, and transition stages, indicating the importance of BMP signaling in amelogenesis (34,35).

In G5 cells, *Bmp2* expression was maintained at a low level during the 14 days of plastic culture (Fig. 2C, left panels), whereas in the collagen culture, the levels were significantly enhanced at day 1, and maintained until day 14. However, both the 3D culture systems demonstrated enhanced *Bmp2* expression in a time-dependent manner. At day 14, *Bmp2* expression showed an increasing trend in the mixed culture compared with the separated culture, which maintained the same level as that on day 7. In

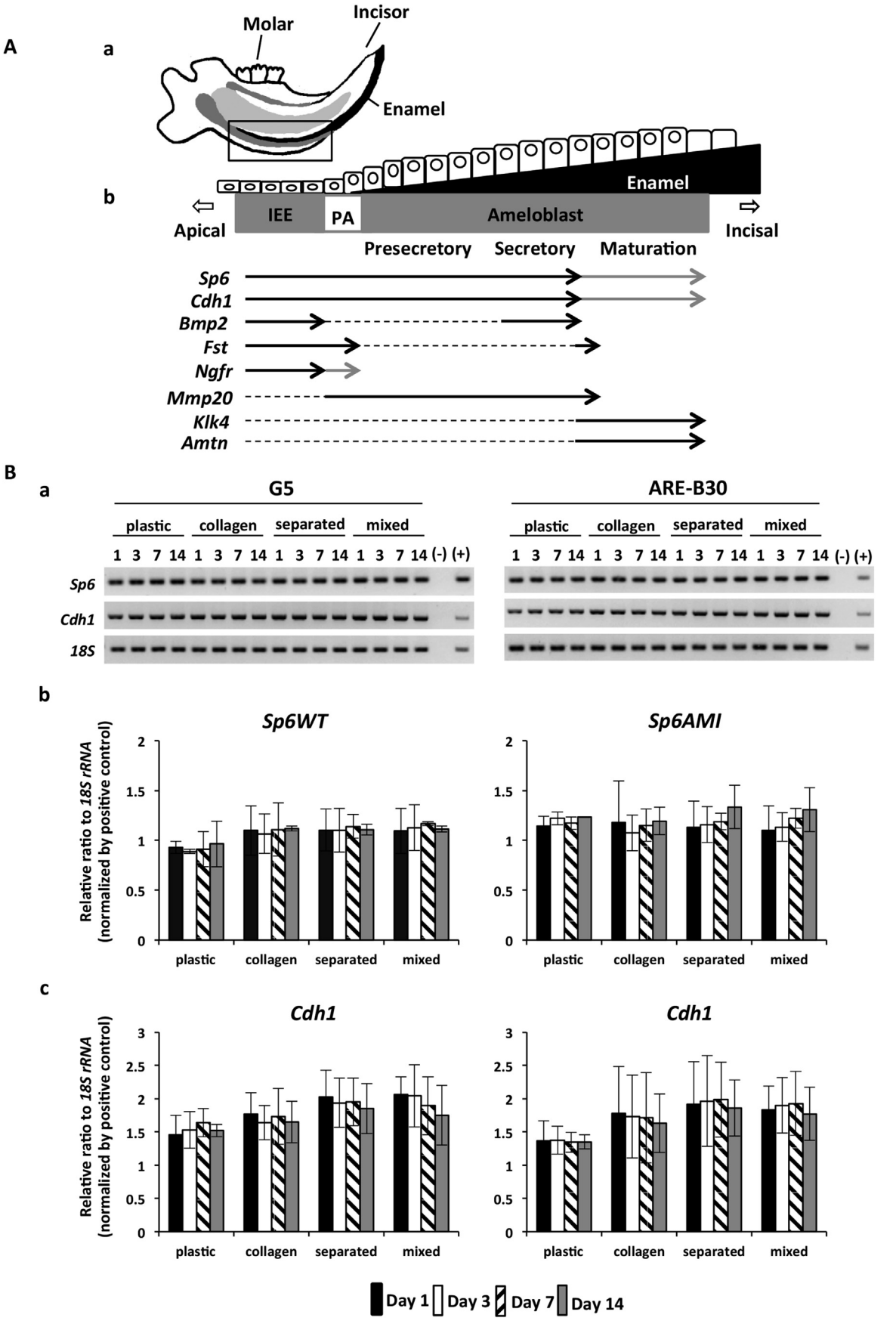

FIG. 2. mRNA expression in the epithelial cells under the various culture conditions. (A) Schematic representation of the stage-specific mRNA expression during ameloblast differentiation *in vivo*. (a) The illustration of rat jaw and teeth (incisor and molars). Black, enamel; dark gray, dental epithelial cells; light gray, pulp. Black box indicates the area which

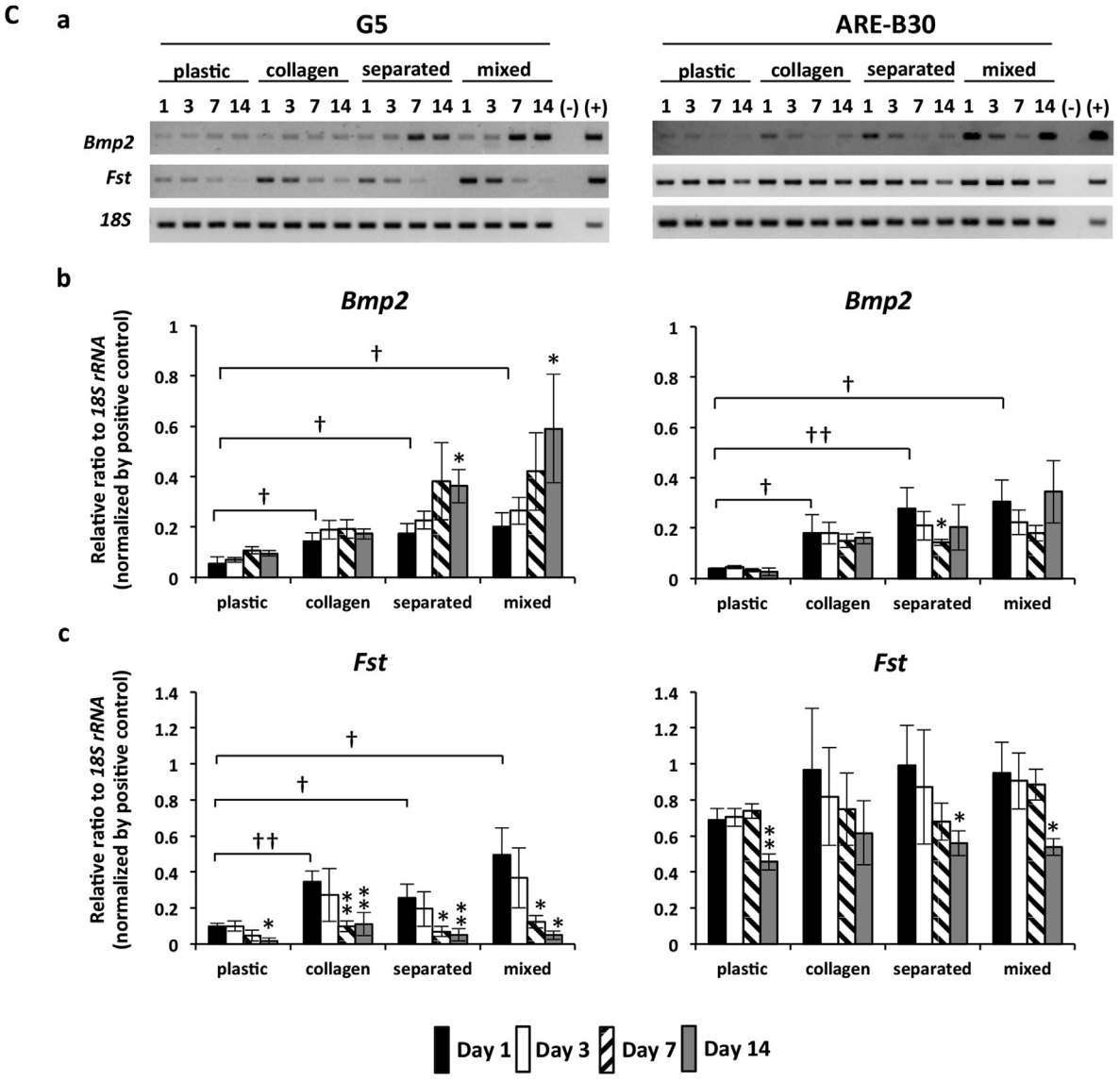

FIG. 2. (*continued*).

contrast, the expression levels of *Bmp2* in the ARE-B30 cells were opposite to that of the G5 cells in the 3D culture systems (Fig. 2C, right panels). Although *Bmp2* levels were enhanced and maintained in the collagen culture, they were found to decrease in a time-dependent manner until day 7 in the 3D culture system. Interestingly, at day 14, the expression levels had returned to those seen on day 1. A similar pattern was observed in the separated and mixed cultures. Taken together, these findings indicate the differences in responsiveness to 3D culture systems between the G5 and ARE-B30 cells.

G5 cells expressed very limited amounts of *Fst* mRNA (Fig. 2C, left panels). Expression levels were enhanced and maintained during the first 3 days on collagen; subsequently, a decrease in levels was observed until day 14 among all the culture systems (Fig. 2C, left panels). Conversely, in the ARE-B30 cells, the basal *Fst* expression level was higher than that in the G5, and was enhanced

enlarged illustration of ameloblast differentiation below. (b) Stage-specific mRNA expression profile during ameloblast differentiation *in vivo*. Black arrows indicate the stages during which each mRNA was expressed as reported in previous studies (18,33–36,45,47,48). Gray arrows indicate predicted mRNA expression based on data from protein expression levels (27,37,49). Dashed lines indicate auxiliary lines to connect the name of the gene with the corresponding black arrow. IEE, inner enamel epithelium; PA, pre-ameloblast. (B) Gene expression levels of dental epithelial markers (*Sp6* and *Cdh1*) in the G5 and ARE-B30 cells. (a) Gene expression was analyzed by RT-PCR. Representative data was shown. Epithelial cells were cultured on plastic, collagen, separated medium, or mixed medium. Numbers indicate the number of days of culture. (−), negative control; (+), positive control. (b) Graphs show the relative levels of *Sp6* expression by densitometric analysis. *Sp6WT*, *Sp6* without mutation; *Sp6AMI*, *Sp6* with mutation. (c) Relative expression levels of *Cdh1*. Black bars, day 1; white bars, day 3; striped bars, day 7; gray bars, day 14. n = 3. (C) mRNA expression of regulatory molecules (*Bmp2* and *Fst*) in G5 and ARE-B30 cells. (a) Gene expression analysis by RT-PCR. (b) Relative expression levels of *Bmp2*. (c) Relative expression levels of *Fst*. All symbols and abbreviations are the same as indicated in panel B. Asterisks indicate significant differences in expression on day 1 versus days 3, 7, and 14 in each culture system. Daggers indicate significant differences between plastic culture and collagen, separated, and mixed cultures on day 1. *p*-value: *, † <0.05; **, †† <0.01; ***, ††† <0.001. (D) mRNA expression levels of the stage-specific markers of ameloblasts (*Ngfr*, *Mmp20*, *Klk4*, and *Amtn*) in G5 and ARE-B30 cells. (a) Gene expression analysis by RT-PCR. Graphs demonstrating relative levels of *Ngfr* (b), *Mmp20* (c), *Klk4* (d), and *Amtn* (e), respectively. All symbols and abbreviations are the same as indicated in panel B. Asterisks (*) indicate significant differences between day 1 and days 3, 7, 14 in each culture system. *p*-value: * <0.05; ** <0.01; *** <0.001; **** <0.0001.

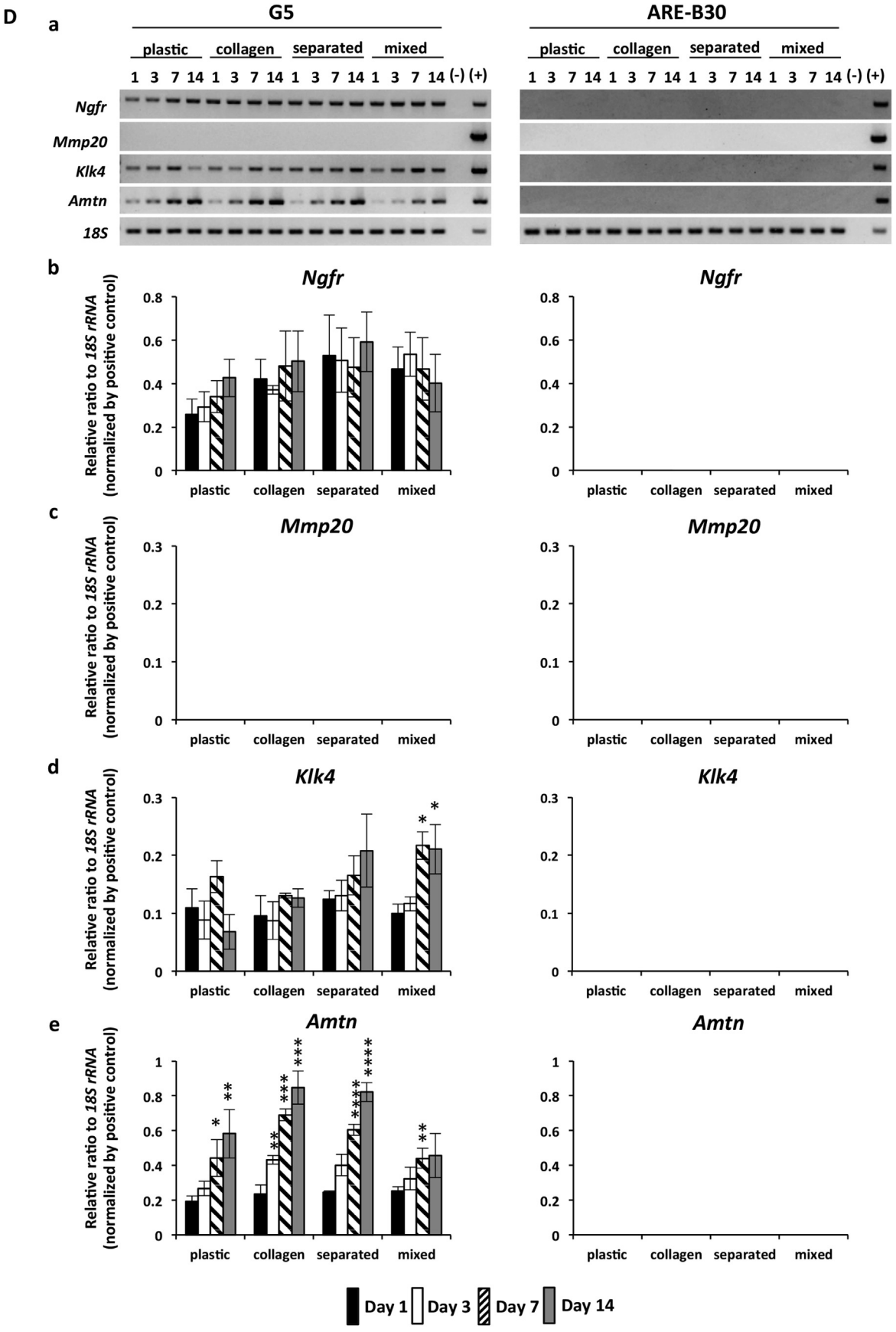

FIG. 2. (*continued*).

by day 1; thereafter, a decreasing tendency in the expression levels was observed in all culture systems (Fig. 2C, right panels). All culture systems presented with clear reciprocal profiles of *Bmp2* and *Fst* expression in the G5, but not ARE-B30 cells.

To further understand the cellular characteristics of G5 and ARE-B30, we examined the stage-specific markers of ameloblasts, including nerve growth factor receptor (*Ngfr*), *Mmp20*, *Klk4*, and *Amtn*. As shown in Fig. 2A, *Ngfr* is expressed at the initiation stage of ameloblast differentiation (36,37), *Mmp20* is expressed at the secretory stage, and *Klk4* and *Amtn* are expressed during the transition to maturation stages of amelogenesis, respectively (12,13). Strikingly, the G5 cells expressed *Amtn*, *Klk4*, and *Amtn*, but not *Mmp20* (Fig. 2D, left panels) in the present study, whereas ARE-B30 cells expressed none of these markers in both 2D and 3D culture systems (Fig. 2D, right panels).

The initiation stage marker, *Ngfr* was stably expressed in the G5 cells in all culture systems. On the other hand, the expression patterns of the maturation stage markers were quite different. *Klk4* expression levels at each time point were varied in the plastic culture when compared to that in the collagen. In the 3D culture systems, *Klk4* expression was significantly enhanced by day 7, and maintained at that level until day 14. Interestingly, the expression pattern of *Amtn*, another late stage marker, was different from that of *Klk4*. *Amtn* expression was significantly enhanced, in a time-dependent manner, in the 2D and 3D culture systems. Collagen culture demonstrated a slight enhancement in the expression levels of *Amtn*, whereas the mixed culture presented with a relatively suppressive pattern. These findings clearly demonstrated the differential responses of the G5 and ARE-B30 cells to the distinct culture systems.

Effect of cell density on the expression levels of ameloblast differentiation markers in G5 cells According to the expression profiles, we found three characteristics of *Amtn* expression. First, *Amtn* was expressed in G5, but not in the ARE-B30 cells. Second, the expression demonstrated a tendency for enhancement in a time-dependent manner. Third, the regulation of *Amtn* expression was not affected in any of the culture conditions. These features suggested that *Amtn* expression might be regulated by cell–cell contact in the G5 cells. To examine this possibility, four different cell-densities of G5 were seeded on the plastic dish and *Amtn* expression was analyzed after culturing for the indicated time points (Fig. 3). *Klk4* expression was analyzed in parallel because of its similarity to *Amtn* as a stage marker *in vivo*.

As shown in Fig. 3A, the G5 cells were seeded on 35 mm plastic dishes at concentrations of 3×10^4, 1×10^5, 3×10^5, and 1×10^6 cells per dish, corresponding to the cellular confluency at 3%, 10%, 30% and 100%, respectively, at day 1. *Amtn* expression was enhanced in a density- and time-dependent manner from day 1 to day 5. In contrast, *Klk4* expression was weakly but distinctly enhanced under the different culturing conditions (Fig. 3B). These findings suggest that the intensity of the cell–cell contact may play a role in regulating *Amtn* and *Klk4* expression.

DISCUSSION

In this study, we applied the *in vitro* 2D and 3D culture systems to analyze defective amelogenesis *in vivo* by comparing two dental epithelial cell types, wild-type G5 versus AMI-derived ARE-B30. Phenotypic screening using these systems identified stage-specific defects in amelogenesis by demonstrating aberrant gene responsiveness in the ARE-B30 cells. Furthermore, these defects were well correlated with *in vivo* AI phenotypes in the AMI rat (17). Fig. 4 summarizes the gene profiles observed in the *in vitro* culture systems, in parallel with the schematic representation of amelogenesis *in vivo*.

The 3D culture system was designed to mimic the initiation stage of amelogenesis, wherein the dental epithelial and mesenchymal cells are separated by a basement membrane (Fig. 4, *in vivo* part) (8). The plastic 2D culture cannot provide a collagen matrix or mesenchymal effects, thereby resembling the maturation stage of amelogenesis. During this stage, *in vivo*, the dental epithelial cells (ameloblasts) are positioned at a distance from the mesenchymal cells (odontoblasts), separated by the self-secreted proteins and partly mineralized tissue (8). Therefore, ameloblasts are attached to the hard surface and potentially stimulated in several ways, including the autocrine and paracrine pathways, cell–cell interaction, and cellular junctional communication through ion exchange (38–40).

In the present study, we found that G5 and ARE-B30 cells stably expressed *Cdh1* and *Sp6* in all culture systems, confirming the epithelial identity of both cells, although the gene status of *Sp6* is different between cell types (Fig. 4, *in vitro* part). Despite the shared epithelial identity, differences in gene regulation between G5 and ARE-B30 cells were clearly visible in the 2D and 3D culture systems.

Reciprocal expression of *Bmp2* and *Fst* was observed in the G5 cells, in consistent with those in the IEE *in vivo* (8,35). In contrast, a decreased tendency in the expression levels of both these genes was observed in the ARE-B30 cells. Notably, ARE-B30 cells presented with higher *Fst* expression levels when compared with G5 cells in all culture systems. Wang et al. (35) reported that dental epithelial cells with high *Fst* expression during the initiation stage do not differentiate into ameloblasts, resulting in the production of enamel free areas. In addition, the basal levels of both *Bmp2* and *Fst* expression were enhanced by collagen culture in the G5 and ARE-B30 cells in the present study. Collagen type I membrane was used as a replacement for the matrix in the basement membrane *in vivo*, which mainly contains collagen type IV during the initiation stage (9). Both types of collagen containing the RGD sequence can bind to the integrin α/β dimer on the epithelial surface (41) and transmit signals by interacting with second messengers, such as tyrosine kinases (FAK, Fyn, and ILK), cytoskeletal proteins, MAP kinases, Rho kinase, and PKB/Akt, in the cytoplasmic region, in order to regulate cell shape and polarity, proliferation, differentiation, and apoptosis (42). Nevertheless, further studies are required to understand the molecular basis for the up-regulation in *Bmp2* and *Fst* expression by collagen type I. Interestingly, *Ngfr*, another IEE marker (36), was expressed at a constant level in the G5 cells, but not in the ARE-B30 cells. *Mmp20*, a marker of the pre-ameloblast to secretory stages (12), was not detected in either of the cell types.

These findings indicate that ARE-B30, along with mutated *Sp6*, might not be committed to ameloblast lineage cells. The intact Sp6 protein function may be required for the cell fate decision of the dental epithelia during the early initiation stage. Sp6 protein expression in the tooth has been reported by two groups using different systems of immunohistochemical analyses. Our group used rat incisor-sections to detect Sp6 protein during the pre-ameloblast to the maturation stages using a peptide antibody designed for the C-terminus of the rat Sp6 (27). The other group analyzed Sp6 expression in the inner dental epithelial layer and secondary enamel knots of mouse molars using a peptide antibody against the N-terminus of the Sp6 (20). The discrepancy in Sp6 detectability between the two reports might be attributed to differences in the species used, the portion of the peptide sequences utilized as antigen, the sensitivity and/or affinity of the antibodies, and the procedure used for antigen retrieval. Consequently, the activity of the Sp6 protein during the initiation stage remains to be confirmed.

Amtn and *Klk4* are expressed during the transition to the maturation stages (8,9), and are known as AI-causative genes (5,43). In the present study, *Amtn* and *Klk4* were detected only in the G5, but not in the ARE-B30 cells. Intriguingly, careful observation revealed that the regulation of *Amtn* was slightly different from

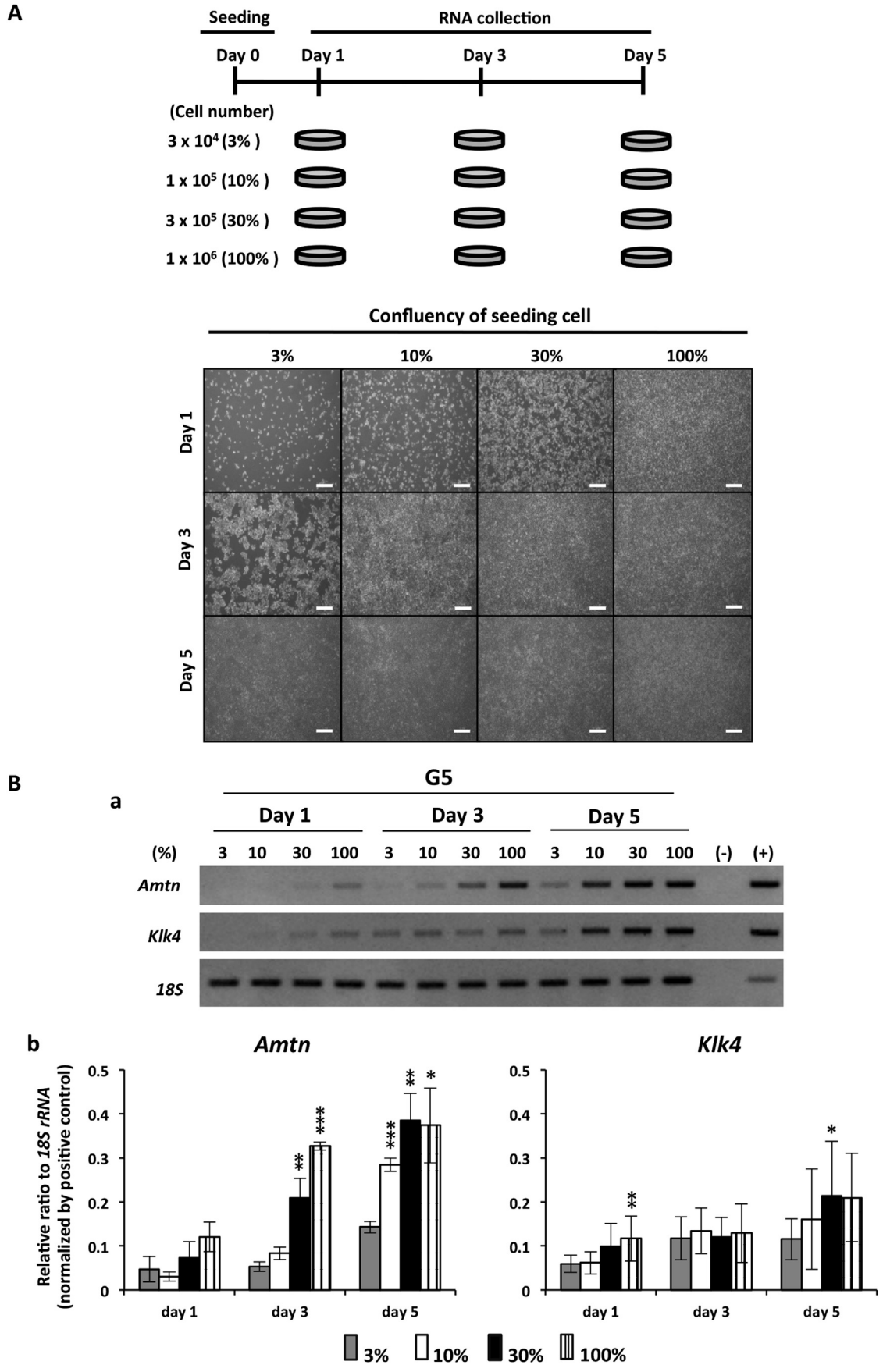

FIG. 3. Effects of cell density on *Amtn* and *Klk4* expression in G5 cells. (A) Experimental design and cell morphology. G5 were seeded in various confluencies (3%, 10%, 30%, and 100%) on each plastic dish. RNA was isolated from the cells at day 1, 3, and 5. Bars indicate 1 mm. (B) *Amtn* and *Klk4* expression in G5 cells. (a) RT-PCR analysis. (−), negative control; (+),

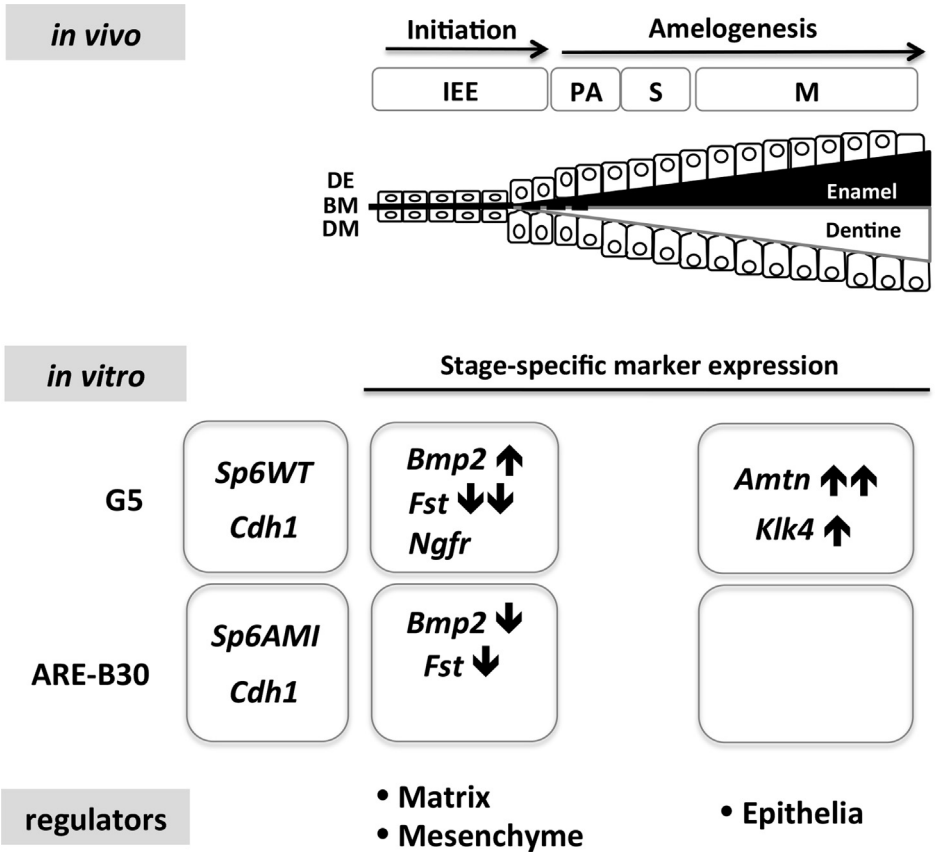

FIG. 4. Summary of phenotypic screening using the 2D and 3D culture systems. Scheme of amelogenesis *in vivo* supplemented with dental mesenchyme. IEE, inner enamel epithelium; PA, pre-ameloblast; S, secretory stage; M, maturation stage. DE, dental epithelial cell; BM, basement membrane; DM, dental mesenchymal cell. Diagram representing summary of stage-specific marker expression in G5 and ARE-B30 cells using the *in vitro* culture systems. Black arrows indicate up-regulated and down-regulated gene expressions. Regulators in stage-specific gene expression.

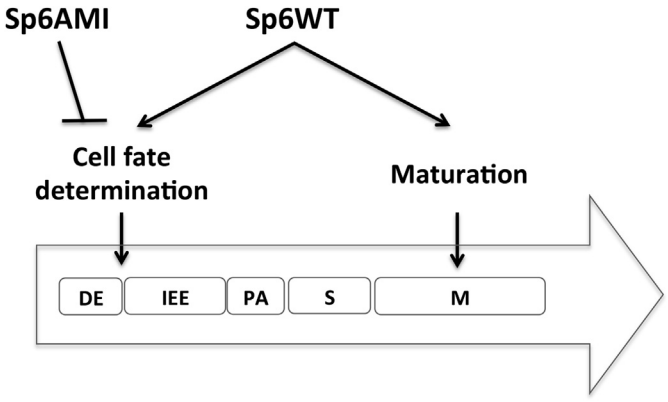

FIG. 5. Diagram illustrating working hypothesis for Sp6 regulation in amelogenesis. Sp6AMI cannot enter the dental epithelial cell lineage due to loss of cell fate determination. DE, dental epithelial cell; IEE, inner enamel epithelium; PA, pre-ameloblast; S, secretory stage; M, maturation stage.

that of *Klk4*. Firstly, *Amtn* expression was enhanced in a time-dependent manner in all the G5 cultures. More importantly, this enhancement was not altered by collagen or mesenchymal regulation, suggesting that the homocytic, cell–cell contact dependent signaling mechanism plays a role in *Amtn* regulation. The importance of epithelial cell–cell contact during ameloblast differentiation has been reported in other *in vitro* culture systems (44). Kawano et al. (44) demonstrated the induction of the secretory stage markers *Amel* and *Ambn* using confluent HAT-7 cells, a dental epithelial cell line derived from the cervical loop of the rat incisor. They also detected a molecular link between cell density and *Notch1* and *Jagged1* expression (44). Furthermore, the mixed culture in the 3D culture system demonstrated relatively reduced levels of *Amtn* expression in the G5 cells, which may be attributed to the dilution of the positive factor(s) secreted by these cells or the effect of inhibitory molecule(s) secreted by RPC-C2A. *Klk4* expression was maintained in the 2D culture systems, and enhanced in both the 3D culture systems with RPC-C2A in the G5 cells, suggesting that *Klk4* expression can be controlled by paracrine effect via mesenchymal factors. The differences in *Amtn* and *Klk4* expression indicate the specificities of gene regulation, although the specific signals involved remain unclear. TGF-beta, a *Klk4* regulator expressed in ameloblasts during amelogenesis, regulates both *Klk4* and *Mmp20* expression in an autocrine or paracrine manner (14). *Mmp20* is expressed during the pre-ameloblast and secretory stages of the ameloblasts; however, the expression levels are lowered after the transition stage (35,45). Interestingly, in the present study, *Mmp20* expression was not detected in the G5 and ARE-B30 cells, suggesting that the culture conditions used in this

positive control. (b) Graphs demonstrate the relative expression levels obtained by densitometric analysis. The levels were normalized to the positive control and then to *18S rRNA*. n = 3. Asterisks (*) indicate significant differences between the 3% and the 10%, 30%, and 100% cell confluencies. *p*-value: * <0.05; ** <0.01; *** <0.001. Gray bars, 3%; white bars, 10%; black bars, 30%; vertical lined bars, 100% confluency at day 1, respectively.

study could not induce the regulatory signal(s) critical for *Mmp20* expression.

The loss of *Amtn* and *Klk4* expression in ARE-B30 cells suggests that normal *Sp6* function may be required for cell fate decision and for the regulation of the expression of both these genes. We have previously reported that *Amtn* expression is down-regulated following *Sp6*-knockdown in the Sp6-stable-transformant C9 cells (25). Furthermore, Amtn is thought to play a role in cell–matrix adhesion and nucleation during mineralization (7,46), which is consistent with the varied cellular structure in the AMI rat: the ameloblasts are histologically disorganized and non-polarized, resulting in perturbed amelogenesis with hypo-mineralization of the enamel (17). Furthermore, using database analysis we have identified that the predicted promoter sequences of *Amtn* and *Klk4* contain GC sequences and several potential Sp1 binding sites (data not shown). These results suggested that both *Amtn* and *Klk4* could be controlled by the transcription factor Sp6.

The current study presents our working hypothesis on the dual roles of Sp6 in amelogenesis (Fig. 5), cell fate determination during the early stage, and control of enamel maturation during the late stage in conjunction with homocytic epithelial cellular regulation. We hypothesized that Sp6-directed ameloblast differentiation enhances the ability to control mineralization of the enamel via *Amtn* and *Klk4* expression, and completes the maturation stage. In contrast, Sp6AMI cannot induce the cells to enter the dental epithelial cell lineage, as shown by the aberrant expression of *Bmp2* and *Fst*, without the expression of additional differentiation markers in the ARE-B30 cells. Further studies are challenged to evaluate and prove this hypothesis.

In conclusion, comparative usage of 2D and 3D culture systems is useful and convenient to distinguish the phenotypic differences between AI-derived ARE-B30 and control G5 cells, and to analyze the causative mechanisms of gene regulation. Based on the findings of this study, we propose dual roles of Sp6 in amelogenesis. Our 2D and 3D culture systems provide a simple platform, *in vitro*, to understand the precise molecular mechanisms of defective amelogenesis caused by mutation of *Sp6 in vivo*.

ACKNOWLEDGMENTS

This work was partly supported by the 2016 Research Award for Oral Sciences from the Graduate School of Oral Sciences, Tokushima University, Japan (DYA), Fellowship from Universitas Muhammadiyah Yogyakarta, Indonesia (DYA), Presidential Research Budget of Tokushima University. We thank the Support Center for Advanced Medical Science in the Faculty of Dentistry at the University of Tokushima for their technical assistance. The authors declare no conflict of interest.

References

1. **Amelian, A., Wasilewska, K., Megias, D., and Winnicka, K.:** Application of standard cell cultures and 3D in vitro tissue models as an effective tool in drug design and development, Pharmacol. Rep., **69**, 861–870 (2017).
2. **Duval, K., Grover, H., Han, L. H., Mou, Y., Pegoraro, A. F., Fredberg, J., and Chen, Z.:** Modeling physiological events in 2D vs. 3D cell culture, Physiology (Bethesda), **32**, 266–277 (2017).
3. **Riedl, A., Schlederer, M., Pudelko, K., Stadler, M., Walter, S., Unterleuthner, D., Unger, C., Kramer, N., Hengstschläger, M., Kenner, L., and other 3 authors:** Comparison of cancer cells in 2D vs 3D culture reveals differences in AKT-mTOR-S6K signaling and drug responses, J. Cell Sci., **130**, 203–218 (2017).
4. **Bloom, A. B. and Zaman, M. H.:** Influence of the microenvironment on cell fate determination and migration, Physiol. Genom., **46**, 309–314 (2014).
5. **Crawford, P., Aldred, M., and Zupan, A.:** Amelogenesis imperfecta, Orphanet. J. Rare. Dis., **2**, 17 (2007).
6. **Witkop, C. J., Jr.:** Hereditary defect in enamel and dentin, Acta Genet., **7**, 236–239 (1957).
7. **Smith, C. E., Poulter, J., Anataviciute, A., Kirkham, J., Brookes, S., Inglehearn, C., and Mighell, A.:** Amelogenesis imperfecta; genes, proteins, and pathways, Front. Physiol., **8**, 435 (2017).
8. **Balic, A. and Thesleff, I.:** Tissue interactions regulating tooth development and renewal, Curr. Top. Dev. Biol., **115**, 157–186 (2015).
9. **Heikinheimo, K. and Salo, T.:** Expression of basement membrane type IV collagen and type IV collagenases (MMP-2 and MMP-9) in human fetal teeth, J. Dent. Res., **74**, 1226–1234 (1995).
10. **Simmer, J. P. and Hu, J. C.:** Dental enamel formation and its impact on clinical dentistry, J. Dent. Educ., **65**, 896–905 (2001).
11. **Robinson, C.:** Enamel maturation: a brief with implications for some enamel dysplasias, Front. Physiol., **5**, 388 (2014).
12. **Lu, Y., Papagerakis, P., Yamakoshi, Y., Hu, J. C., Bartlett, J. D., and Simmer, J. P.:** Functions of KLK4 and MMP-20 in dental enamel formation, Biol. Chem., **389**, 695–700 (2008).
13. **Moffatt, P., Smith, C. E., St-Arnaud, R., Simmons, D., Wright, J. T., and Nanci, A.:** Cloning of rat amelotin and localization of the protein to the basal lamina of maturation stage ameloblasts and junctional epithelium, Biochem. J., **399**, 37–46 (2006).
14. **Kobayashi-Kinoshita, S., Yamakushi, Y., Onuma, K., Yammamoto, R., and Asada, Y.:** TGF-β1 autocrine signaling and enamel matrix components, Sci. Rep., **6**, 3364 (2016).
15. **Fouillen, A., Dos Santos Neves, J., Mary, C., Castonguay, J. D., Moffatt, P., Baron, C., and Nanci, A.:** Interactions of AMTN, ODAM and SCPPPQ1 proteins of a specialized basal lamina that attaches epithelial cells to tooth mineral, Sci. Rep., **7**, 46683 (2017).
16. **Ishibashi, K., Iino, T., and Sekiguchi, F.:** Amelogenesis imperfecta, a new dental mutation in rats, Lab. Anim. Sci., **40**, 16–20 (1990).
17. **Muto, T., Miyoshi, K., Hoiguchi, T., Hagita, H., and Noma, T.:** Novel genetic linkage of rat *Sp6* mutation to Amelogenesis imperfecta, Orphanet. J. Rare Dis., **7**, 34 (2012).
18. **Nakamura, T., Unda, F., Vega, S., Vilaxa, A., Fukumoto, S., Yamada, K., and Yamada, Y.:** The Kruppel-like factor epiprofin is expressed by epithelium of developing teeth, hair follicles, and limb buds and promotes cell proliferation, J. Biol. Chem., **279**, 626–634 (2004).
19. **Hertveldt, V., Louryan, S., Reeth, T., Dreeze, P., Vooren, P., Szpirer, J., and Szpirer, J.:** The development of several organs and appendages is impaired in mice lacking Sp6, Dev. Dyn., **237**, 883–892 (2008).
20. **Nakamura, T., de Vega, S., Fukumoto, S., Jimenez, L., Unda, F., and Yamada, Y.:** Transcription factor epiprofin is essential for tooth morphogenesis by regulating epithelial cell fate and tooth number, J. Biol. Chem., **283**, 4825–4833 (2008).
21. **Muto, T., Miyoshi, K., Horiguchi, T., and Noma, T.:** Dissection of morphological and metabolic differentiation of ameloblasts via ectopic SP6 expression, J. Med. Invest., **59**, 59–68 (2012).
22. **Adiningrat, A., Tanimura, A., Miyoshi, K., Hagita, H., Yanuaryska, R. D., Arinawati, D. Y., Horiguchi, T., and Noma, T.:** Isolation and characterization of dental epithelial cells derived from amelogenesis imperfecta rat, Oral Dis., **22**, 132–139 (2016).
23. **Abe, K., Miyoshi, K., Muto, T., Ruspita, I., Horiguchi, T., Nagata, T., and Noma, T.:** Establishment and characterization of rat dental epithelial derived ameloblast lineage clones, J. Biosci. Bioeng., **103**, 479–485 (2007).
24. **Wahyudi, I. A., Horiguchi, T., Miyoshi, K., Muto, T., Utami, T. W., Hagita, H., and Noma, T.:** Isolation and characterization of mouse specificity protein 6 promoter, Indones. J. Dent. Res., **1**, 21–34 (2010).
25. **Utami, T. W., Miyoshi, K., Hagita, H., Yanuaryska, R. D., Horiguchi, T., and Noma, T.:** Possible linkage of Sp6 transcriptional activity with amelogenesis by protein stabilization, J. Biomed. Biotechnol., **2011**, 320987 (2011).
26. **Adiningrat, A., Tanimura, A., Miyoshi, K., Yanuaryska, R. D., Hagita, H., Horiguchi, T., and Noma, T.:** Ctip2-mediated *Sp6* transcriptional regulation in dental epithelium-derived cells, J. Med. Invest., **61**, 126–136 (2014).
27. **Ruspita, I., Miyoshi, K., Muto, T., Abe, K., Horiguchi, T., and Noma, T.:** Sp6 downregulation of follistatin gene expression in ameloblasts, J. Med. Invest., **55**, 87–98 (2008).
28. **Yanuaryska, R. D., Miyoshi, K., Adiningrat, K., Horiguchi, T., Tanimura, A., Hagita, H., and Noma, T.:** Sp6 regulation of *Rock1* promoter activity in dental epithelial cells, J. Med. Invest., **61**, 306–317 (2014).
29. **Otsu, K., Kishigami, R., Fujiwara, N., Ishizeki, K., and Harada, H.:** Functional role of Rho-kinase in ameloblast differentiation, J. Cell. Physiol., **226**, 2527–2534 (2011).
30. **Kasugai, S., Adachi, M., and Ogura, H.:** Establishment and characterization of a clonal cell line (RPC-C2A) from dental pulp of the rat incisor, Arch. Oral Biol., **33**, 887–891 (1988).
31. **Matsumoto, A., Harada, H., Saito, M., and Taniguchi, A.:** Induction of enamel matrix protein protein expression in an ameloblast cell line co-cultured with a mesenchymal cell line in vitro, In vitro Cell. Dev. Biol. Anim., **47**, 39–44 (2011).
32. **Ueno, A., Yamashita, K., Miyoshi, K., Horiguchi, T., Ruspita, I., Abe, K., and Noma, T.:** Soluble matrix from osteoblastic cells induces mineralization by dental pulp cells, J. Med. Invest., **53**, 297–302 (2006).

33. **Terling, C., Heymann, R., Rozell, B., Obrink, B., and Wroblewski, J.:** Dynamic expression of E-cadherin in ameloblasts and cementoblasts in mice, Eur. J. Oral Sci., **106**, 137–142 (1998).
34. **Aberg, T., Wozney, J., and Thesleff, I.:** Expression patterns of bone morphogenetic proteins (*Bmps*) in the developing mouse tooth suggest roles in morphogenesis and cell differentiation, Dev. Dyn., **210**, 383–396 (1997).
35. **Wang, X. P., Suomalainen, M., Jorgez, C. J., Matzuk, M. M., Werner, S., and Thesleff, I.:** Follistatin regulates enamel patterning in mouse incisors by asymmetrically inhibiting BMP signaling and ameloblast differentiation, Dev. Cell, **7**, 719–730 (2004).
36. **Byers, M. R., Schatteman, G. C., and Bothwell, M.:** Multiple functions for NGF receptor in developing, aging and injured rat teeth are suggested by epithelial, mesenchymal and neural immunoreactivity, Development, **109**, 461–471 (1990).
37. **Kawano, S., Saito, M., Handa, K., Morotomi, T., Toyono, T., Seta, Y., Nakamura, N., Uchida, T., Toyoshima, K., Ohishi, M., and Harada, H.:** Characterization of dental epithelial progenitor cells derived from cervical loop epithelium in a rat lower incisor, J. Dent. Res., **83**, 129–133 (2004).
38. **Bei, M.:** Molecular genetics of ameloblast cell lineage, J. Exp. Zool. B Mol. Dev. Evol., **312B**, 437–444 (2009).
39. **Bartlett, J. D. and Smith, C. E.:** Modulation of cell-cell junctional complexes by matrix metalloproteinases, J. Dent. Res., **92**, 10–17 (2013).
40. **Bronckers, A. L.:** Ion transport by ameloblasts during amelogenesis, J. Dent. Res., **96**, 243–253 (2017).
41. **Barczyk, M., Carracedo, S., and Gullberg, D.:** Integrins, Cell Tissue Res., **339**, 269–280 (2010).
42. **Legate, K. R., Wickström, S. A., and Fässler, R.:** Genetic and cell biological analysis of integrin outside-in signaling, Genes Dev., **23**, 397–418 (2009).
43. **Smith, C., Murillo, G., Brookes, S., Poulter, J., Silva, S., Jennifer, K., Inglehearn, C., and Mighell, A.:** Deletion of amelotin exons 3-6 is associated with amelogenesis imperfecta, Hum. Mol. Genet., **25**, 3578–3587 (2016).
44. **Kawano, S., Morotomi, T., Toyono, T., Nakamura, N., Uchida, T., Ohishi, M., Toyoshima, K., and Harada, H.:** Establishment of dental epithelial cell line (HAT-7) and the cell differentiation dependent on Notch signaling pathway, Connect. Tissue Res., **43**, 201–211 (2002).
45. **Hu, J. C., Sun, X., Zhang, C., Liu, S., Bartlett, J. D., and Simmer, J. P.:** Enamelysin and kallikrein-4 mRNA expression in developing mouse molars, Eur. J. Oral Sci., **110**, 307–315 (2002).
46. **Abbarin, N., San Miguel, S., Holcroft, J., Iwasaki, K., and Ganss, B.:** The enamel protein amelotin is a promoter of hydroxyapatite mineralization, J. Bone Miner. Res., **30**, 775–785 (2015).
47. **Heikinheimo, K., Bègue-Kirn, C., Ritvos, O., Tuuri, T., and Ruch, J. V.:** The activin-binding protein follistatin is expressed in developing murine molar and induces odontoblast-like cell differentiation in vitro, J. Dent. Res., **76**, 1625–1636 (1997).
48. **Iwasaki, K., Bajenova, E., Somogyi, E., Miller, M., Nguyen, V., Nourkeyhani, H., Gao, Y., Wendel, M., and Ganss, B.:** Amelotin—a novel secreted, ameloblast-specific protein, J. Dent. Res., **84**, 1127–1132 (2005).
49. **Sorkin, B. C., Wang, M. Y., Dobeck, J. M., Albergo, K. L., and Skobe, Z.:** The cadherin-catenin complex is expressed alternately with the adenomatous polyposis coli protein during rat incisor amelogenesis, J. Histochem. Cytochem., **48**, 397–406 (2000).